A new look at southeast Greenland barrier winds and katabatic flow

Kent Moore[1] and Ian Renfrew[2]

[1]University of Toronto, Canada
[2]University of East Anglia, UK

Although the seas around southeast Greenland have been known to be a hazard to maritime traffic as a result of the high winds that occur in the region, including the sinking of the MS Hans Hedtoft with the loss of 95 lives in a northeasterly gale near Cape Farewell during January 1959 (Hocking 1969; Rasmussen 1989), Doyle and Shapiro (1999) were the first to provide a quantitative description of a high-speed surface wind system in the region. Using an idealized model of flow past an obstacle similar to Greenland and case studies of the two observed events, they identified a shallow orographic jet, that they referred to as a tip jet, characterized by westerly surface winds in excess of 30 m/s that formed to the east of Cape Farewell. Moore (2003) used the NCEP Reanalysis to show that the surface wind field in the vicinity of Cape Farewell was bimodal in nature with the possibility of both high-speed westerly or easterly winds that were subsequently referred to by Renfrew et al. (2009) as either westerly tip jets, the sort identified by Doyle and Shapiro (1999), or easterly tip jets. In addition, Moore (2003) showed that both classes of tip jets were associated with the interaction of extra-tropical cyclones with the high topography of southern Greenland.

Moore and Renfrew (2005) used scatterometer winds from the QuikSCAT satellite to confirm the earlier results, to provide first-order dynamical explanations, and to further show that the southeast coast of Greenland was a region where high-speed northeasterly surface flow occurred, i.e., barrier flow. Subsequently a global climatology of QuikSCAT winds indicated that the southeast coast of Greenland was in fact the windiest location on the ocean's surface (Sampe and Xie 2007). Local maxima in the occurrence frequency of barrier winds were identified in the QuikSCAT data (Moore and Renfrew 2005) in regions referred to as Denmark Strait North (DSN) and Denmark Strait South (DSS); and diagnosed more clearly in Moore (2012). Harden and Renfrew (2012) noted that these maxima were collocated with steep coastal topography and demonstrated, through idealized simulations, that the enhanced wind speeds in these regions were the result of cross-isobar acceleration arising from the deceleration of the flow impinging on these topographic barriers. Thus these local maxima are examples of so-called corner jets that in the Northern Hemisphere result in an acceleration of the wind to the left of the barrier (Barstad and Gronas 2005).

Southeast Greenland also experiences strong outflow wind events that are triggered by radiative cooling over the central Greenland Ice Sheet (Rasmussen 1989; Heinemann 1999). These katabatic wind events can become channeled down the steep topography of the large fjord systems in the region, most notably the Sermilik and Kangerdlugssuaq Fjords, resulting in high-speed wind events along the coast, known locally as piteraqs (Rasmussen 1989). In February 1970, a piteraq with wind speeds estimated to be in excess of 90 m/s (the last recordings on the town's anemometer before it was destroyed indicated mean winds of 54 m/s with gusts to 70 m/s) devastated the small town of Tasiilaq situated near the mouth of the Sermilik Fjord (Cappelen et al. 2001).

This exceptional event was associated with a deep low-pressure system over the Denmark Strait and it has been proposed that its severity was the result of the compounding effects of the drainage flow off the ice sheet and the northwesterly flow that occurred after the low's passage (Cappelen et al. 2001). The important role that cyclones play in severe piteraqs was subsequently confirmed in a number of case studies (Klein and Heinemann 2002; Mills and Anderson 2003) as well as in a climatology of these events in the vicinity of the Sermilik Fjord (Oltmanns et al. 2014).

Cape Farewell tip jets, southeast Greenland barrier winds, and katabatic flow all play an important role in the regional weather and climate (Renfrew et al. 2008; Harden et al. 2011; Oltmanns et al. 2014). In addition, the elevated air-sea fluxes of heat, moisture, and momentum associated with these wind events impact the regional surface oceanography (Haine et al. 2009; Daniault et al. 2011) as well as contributing to the lower limb of the Atlantic Meridional Overturning Circulation (AMOC). In particular, the elevated air-sea heat fluxes associated with westerly Cape Farewell tip jets and northwesterly katabatic flow have been proposed to be the atmospheric forcing that drives the formation of Labrador Sea Water in the Irminger Sea, an important component of the AMOC (Pickart et al. 2003a; Pickart et al. 2003b; Våge et al. 2009; Oltmanns et al. 2014).

Straneo et al. (2010) argued that barrier flow is important in the exchange of water between fjords and the open ocean along the southeast coast of Greenland. Through this process, it is hypothesized that barrier flow has contributed to the recent presence of warm subtropical waters in these fjords that has been argued to play a role in the recent rapid retreat of the outlet glaciers in the region (Howat et al. 2011). Katabatic flow can also act to advect sea ice away from the coast resulting in the formation of polynyas (Bromwich and Kurtz, 1984) that can have an impact on the ecology of the region (Arrigo 2007). These strong outflow winds can also result in the removal of a fjord's ice mélange, a mixture of sea ice and icebergs that inhibits glacier calving, thereby contributing to the destabilization of glaciers in the region (Amundson et al. 2010, Howat et al. 2011; Walter et al. 2012; Oltmanns et al. 2014).

Southeast Greenland is a data sparse and remote region with limited surface and upper-air observations, making it a challenge to investigate the structure and dynamics of these weather systems and their impact on the coupled climate system. In addition, coastal settlements, where observations are typically made, are usually situated in locations where the topography results in relatively benign microclimates that may not be representative of surrounding regions (Cappelen et al. 2001; Oltmanns et al. 2014). For example the DMI weather station at Tasiilaq, the settlement closest to the Sermilik Fjord, has a mean winter wind speed of 2.6 m/s with a directional constancy of 0.23; while the automatic weather station situated approximately 16 km away, inside the fjord, has a winter mean wind speed of 5.2 m/s with a directional constancy of 0.74 (Oltmanns et al. 2014). Scatterometer winds can provide information on the surface expression of these weather systems over the open ocean (Moore and Renfrew 2005) but provide no information over sea ice or over land. As a result, atmospheric reanalyses – the assimilation of meteorological observations into a consistent numerical weather prediction model – provide a representation of the atmosphere that is suitable for the analysis of climate variability in such an area (Moore, 2003; Våge et al. 2009; Harden and Renfrew 2012; Moore 2012; Oltmanns et al. 2014).

However all these weather systems are mesoscale phenomena that have horizontal length scales on the order of 200-400 km (Moore and Renfrew 2005; Renfrew et al. 2008; Oltmanns et al. 2014). As a consequence, they may be poorly-resolved in most global reanalysis products that typically have effective horizontal resolutions on the order of 400 km or greater (Condron and Renfrew 2013; Laffineur et al. 2014). This is consistent with the results of Duvivier and Cassano (2013), who argued that Weather Research and Forecasting (WRF) model simulations with horizontal resolutions of 50 km or greater under-represented the evolution of Greenland tip jets and barrier flow as well as their air-sea fluxes.

As a consequence, there is a clear need to develop climatologies of these weather systems with sufficient horizontal resolution to capture their fine scale structure. The recent completion of the Arctic System Reanalysis (ASR; Bromwich et al., 2014) that uses the Polar WRF regional forecast model to generate a regional reanalysis of the Arctic and that has a horizontal resolution of either 15 km or 30 km offers the possibility of achieving this goal.

In this article, we compare and contrast the representation of barrier winds and katabatic flow along the southeast coast of Greenland in the Interim Reanalysis from the ECMWF (ERA-I), a typical latest generation global atmospheric reanalysis (Dee et al. 2011), with that from the ASR. These two reanalyses are the result of very different data assimilation systems and underlying numerical models with differing numerical cores, parameterizations, and resolutions. For example, the ERA-I is based on a global spectral model and a highly-advanced 4D variational data assimilation scheme; while the ASR is based on a regional gridpoint model and a 3D variational data assimilation scheme that is optimized for use at high latitudes (Dee et al. 2011; Bromwich et al. 2014). Among these optimizations are the use of a land-surface scheme that includes the implementation of fractional sea ice cover with variable thickness and snow cover as well as an improved representation of the albedo of snow and ice (Bromwich et al. 2014). One point of commonality between the two is that the ERA-I is used to provide initial and lateral boundary conditions for the ASR (Bromwich et al. 2014). The interim version of the ASR that will be used in the article covers the period from 1 January 2000 to 31 December 2010 at a horizontal grid resolution of 30 km resulting in an effective horizontal resolution of ~200 km, i.e., 5-7 times the nominal grid resolution (Skamarock 2004). The ERA-I has a horizontal grid resolution of 0.75° implying an effective horizontal resolution of ~400 km.

A comparison with surface and upper-air data for the one year period from December 2006 to November 2007 indicated that the annual mean biases in surface meteorological fields in the ERA-I and ASR are comparable but that the ASR typically has smaller root mean square errors and higher correlations (Bromwich et al. 2014). A comparison of radiosonde and dropsonde data collected during a mesoscale cyclogenesis event over the Iceland Sea that was investigated during the Greenland Flow Distortion Experiment (Renfrew et al. 2008) indicated

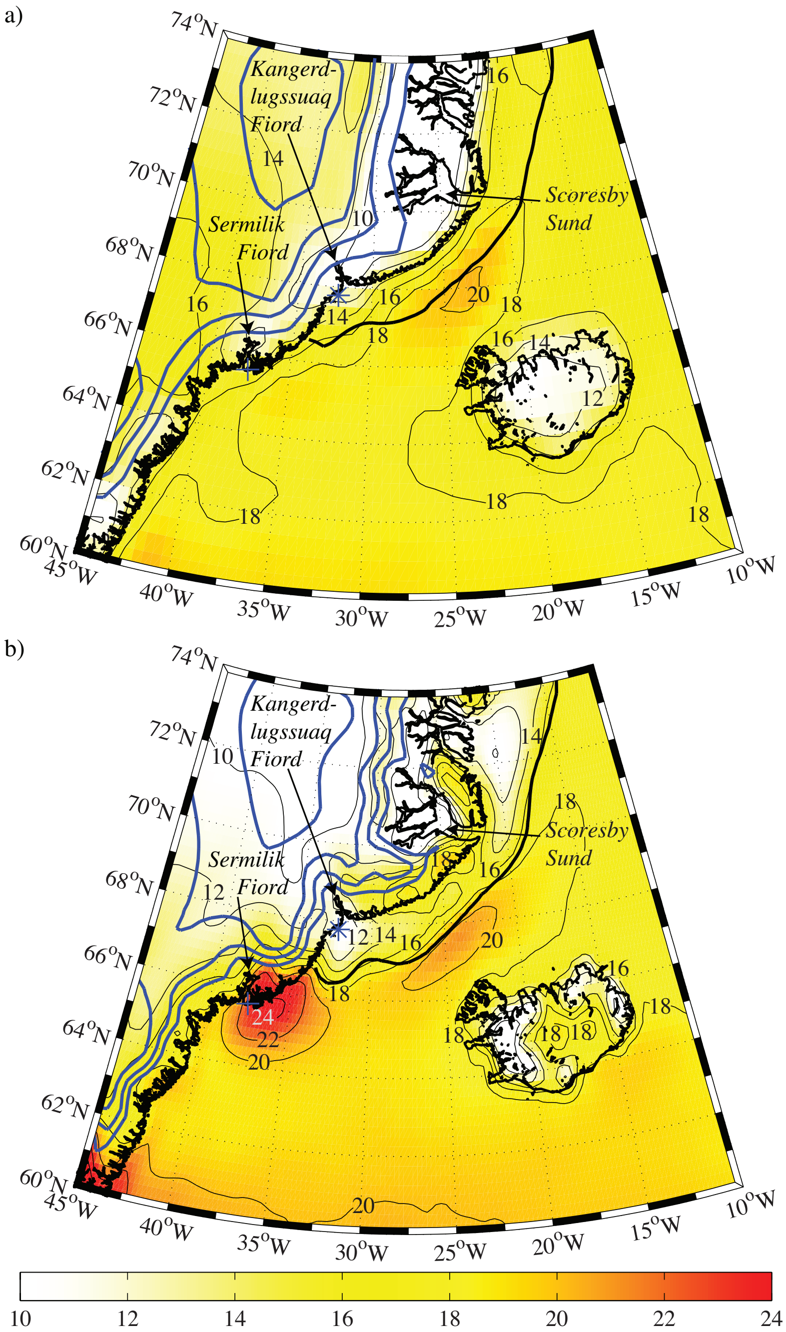

Fig. 1 The 95th percentile 10 m wind speed (m/s) during winter (DJF) 2000-2010 as represented in the: (a) ERA-I and (b) ASR-I. The thick black line represents the winter mean 50% sea ice concentration contour in the respective reanalyses. The thick blue lines represent the 1500, 2500, 3000, and 3500 m height contours in the respective analyses. The major fjords along the southeast coast of Greenland are indicated. The '*' and '+' represent the locations of the DMI weather stations at Aputiteeq and Tasiilaq respectively.

that the ASR typically had a reduced extremal bias in wind speed throughout the troposphere as compared to the ERA-I (Bromwich et al. 2014).

Figure 1 shows the 95th percentile 10 m wind speed from both the ERA-I and ASR-I during the winter months (DJF) for the period of overlap, i.e., 2000-2010. In general, the ASR-I field has more spatial structure as compared to that from the ERA-I. Over the Greenland Ice Sheet and the sea ice along its southeast coast, the 95th percentile wind speeds are generally higher in the ERA-I as compared to the ASR-I. In addition, the gradient across the marginal ice zone is generally more pronounced in the ASR-I. This is most evident in the vicinity of the Denmark Strait where there is a local maximum in the 95th percentile wind speeds present in both reanalyses. In the ERA-I, this maximum is quite diffuse and extends over the sea ice; while in the ASR-I it is focused over the open water. The gradient in the wind speed across the ice edge is most likely the result of the rougher surface of the sea ice as compared to the open ocean (Liu et al., 2006; Petersen and Renfrew 2009). It is likely that the ASR-I with its higher effective spatial resolution is able to better resolve this gradient. The 95th percentile wind speeds in the ASR-I are also significantly higher than those in the ERA-I in the vicinity of the Sermilik Fjord. The same is also true over east Greenland in the vicinity of Scoresby Sund, where there are a number of local maxima present in the ASR-I that are absent in the ERA-I. Finally the ASR-I captures more detail regarding the topographic flow distortion due to Iceland than does the ERA-I.

The diagnostic presented in Figure 1 clearly demonstrates the wealth of additional detail regarding the impact that the high topography of Greenland has on the surface flow in the region that is contained in the ASR-I as compared to the ERA-I. However it does not allow for a partition of the associated high-speed wind events into barrier and katabatic flow. This is possible if one takes into account the distinct directionality of barrier flow, i.e., along the barrier, in this case northeasterly (Moore and Renfrew 2005), and that of katabatic flow, i.e., down-slope, in this case northwesterly

(Oltmanns et al. 2014). Figure 2 shows the occurrence frequency of high-speed northeasterly and northwesterly surface flow during the winter months as represented in the ERA-I and ASR-I. The threshold criterion for high-speed northeasterly flow was set at 15 m/s, while that for northwesterly flow was set at 10 m/s. These thresholds were chosen partly based on wind climatologies. The former captures details of the barrier flow while the latter threshold was also used by Oltmanns et al. (2014) in their definition of katabatic flow events at Sermilik Fjord as represented in the ERA-I.

With regard to barrier flow (i.e., northeasterly high-speed winds), both the ERA-I (Fig. 2a) and ASR-I (Fig. 2b) capture the DSN and DSS locations along the southeast coast of Greenland where high-speed barrier winds are common (Moore and Renfrew 2005). As discussed by previous authors (Harden and Renfrew 2012; Moore 2012), the DSN location is in the vicinity of the steep coastal topography to the north, i.e., upwind, of the Kangerdlugssuaq Fjord with the DSS location is in the vicinity of a similar topographic barrier to the north of the Sermilik Fjord. The DSN maximum in the ASR-I is located over the open water with an enhanced gradient along the ice edge along with an extension inland over the steep topography just to the south of Scoresby Sund, while this maximum is more diffuse in the ERA-I. The occurrence frequencies in the DSS location are considerably higher in the ASR-I and have a pronounced inland extension over the steep coastal topography to the north of Sermilik Fjord. Both of these landward extensions of high-speed barrier flow are consistent with notion that these maxima are the result of 'left-handed' corner jets forced by these topographic barrier (Barstad and Gronas 2005). There is also a similar corner jet present along the southeast coast of Iceland that is better resolved in the ASR-I.

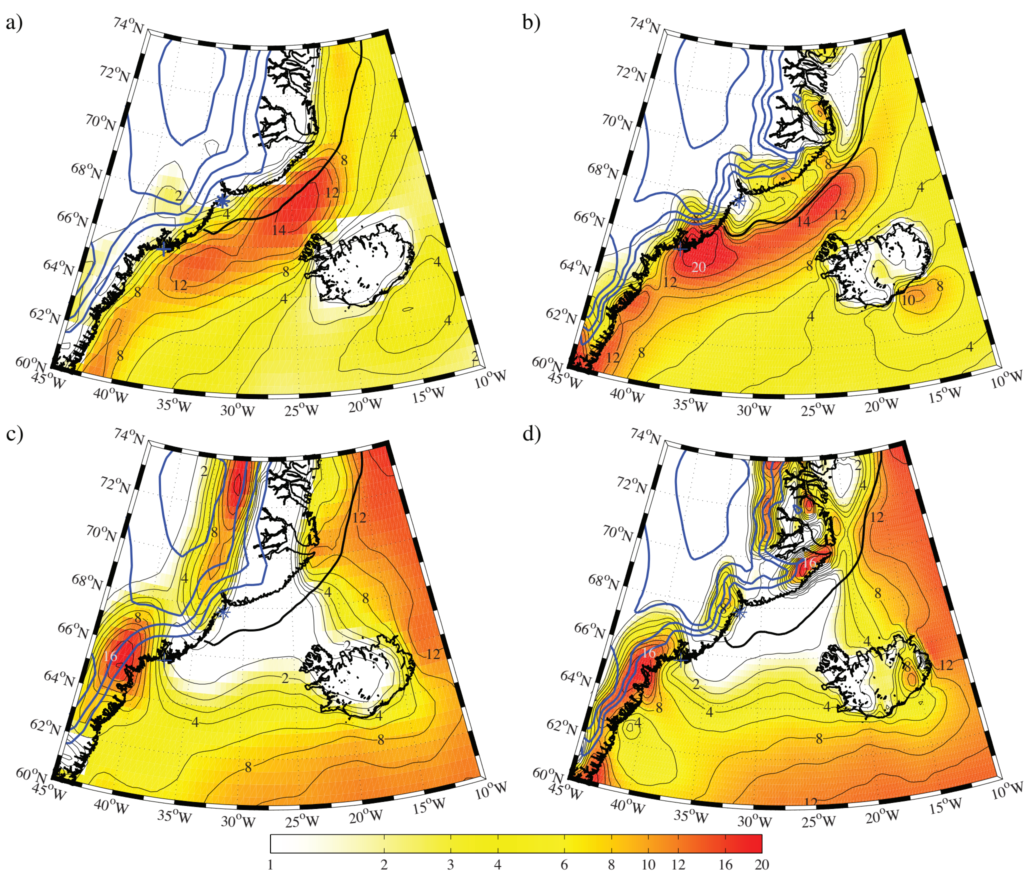

Fig. 2 The frequency of occurrence (%) of northeasterly 10m winds in excess of 15 m/s during the winter (DJF) 2000-2000 as represented in the: (a) ERA-I and (b) ASR-I. The frequency of occurrence (%) of northwesterly 10m winds in excess of 10 m/s during the winter (DJF) 2000-2000 as represented in the: (c) ERA-I and (d) ASR-I. The thick black line represents the winter mean 50% sea ice concentration contour in the respective reanalyses. The thick blue lines represent the 1500, 2500, 3000, and 3500 m height contours in the respective analyses. The '*' and '+' represent the locations of the DMI weather stations at Aputiteeq and Tasiilaq respectively.

Turning our attention to the katabatic winds (i.e., northwesterly flow), one again sees that there is more detail in the ASR-I (Fig. 2d) as compared to that from the ERA-I (Fig. 2c). Along the steep topographic gradient to the east of the Greenland's North Dome, the ERA-I has an extended quasi-linear region where there is an elevated occurrence frequency for high-speed northwesterly flow. The feature extends southwards to the Kangerdlugssuaq Fjord and represents the tendency for the katabatic flow to flow down the topographic gradient (Rasmussen 1989). In the ASR-I this feature is broken into two distinct segments by the topographic ridge to the south of Scoresby Sund, a feature that is not well represented in the ERA-I. The coastal terminus of this ridge, in agreement with Rasmussen (1989), is also a region where the ASR-I indicates that katabatic flow occurs. Both reanalyses indicate that the highest occurrence frequency for katabatic flow occurs to the south of Sermilik Fjord near 65°N 40°W. As was the case farther north, the ASR-I is better able to capture the minimum in the occurrence frequency that occurs along the topographic ridge separating the Kangerdlugssuaq and Sermilik Fjords. This southern maximum for katabatic flow, which is in the vicinity of the large Ikertivaq and Koge Bugt Fjords (Murray et al. 2010), has a pronounced offshore extension as was found to be the case for composite katabatic flow at Sermilik Fjord (Oltmanns et al. 2014). Such an extension is not evident in the vicinity of the Kangerdlugssuaq Fjord, most likely as a result of the increase in roughness over the sea ice.

In the vicinity of the major fjord systems along Greenland's southeast coast, both reanalyses have comparable occurrence frequencies of northwesterly flow with wind speeds in excess of 10 m/s. As discussed by Oltmanns et al. (2014), the ERA-I (and by extension the ASR-I) underestimates the wind speeds during these outflow events. The similarity in behavior between the two reanalyses in this regard suggests that both are resolving the density-driven component of the flow but even the 30 km resolution of the ASR-I is not sufficient to fully capture the acceleration due to the channeling of the flow down these fjord systems. This is consistent with high-resolution modeling of piteraqs in the Sermilik Fjord (M. Oltmanns, pers. comm.).

Both reanalyses also capture the two distinct local maxima in the occurrence of katabatic flow, one to the south of the Sermilik Fjord and the other to the north of Scoresby Sund. The latter is easily understandable as being the result of the steepness of the ice sheet in this region that is the result of the high topography of the North Dome. Topographic gradients are not as large in the vicinity of the southern maximum and in addition, the occurrence frequency is diminished to the north. It is probable that the confluence associated with the topographic saddle point (between the North and South Domes) contributes to the southern maximum, but it is also likely that the impact of northwesterly flow behind cyclones, which are more common farther south (Hoskins and Hodges 2002), also plays a role in the location of this maximum. In this regard, the relative minimum in katabatic flow occurrence in the vicinity of the Kangerdlugssuaq Fjord may also be the result of the infrequent occurrence of cyclones to the north of this fjord.

It is of course important to validate the winds from any reanalysis, especially in topographically complex and data sparse regions such as the southeast coast of Greenland. This is a challenge because, as mentioned previously, the limited observations in the region may exhibit a 'fair weather' bias (Cappelen et al. 2001; Oltmanns et al. 2014). This problem can be illustrated through a comparison of the 10 m wind speed from both the ERA-I and ASR-I at the weather stations near the mouths of the Kangerdlugssuaq Fjord, the Aputiteeq station, and the Sermilik Fjord, the Tasiilaq station. For both stations, the correlation coefficient between the observed wind speeds and those from both reanalysis during the winter are on the order of 0.5. Consideration of the directionality of the observed and reanalysis winds lead to smaller correlation coefficients. Given these results, it is difficult to see how such data can be used to validate the reanalysis winds. There is nevertheless evidence that, at least on the regional scale, that the ASR-I is better

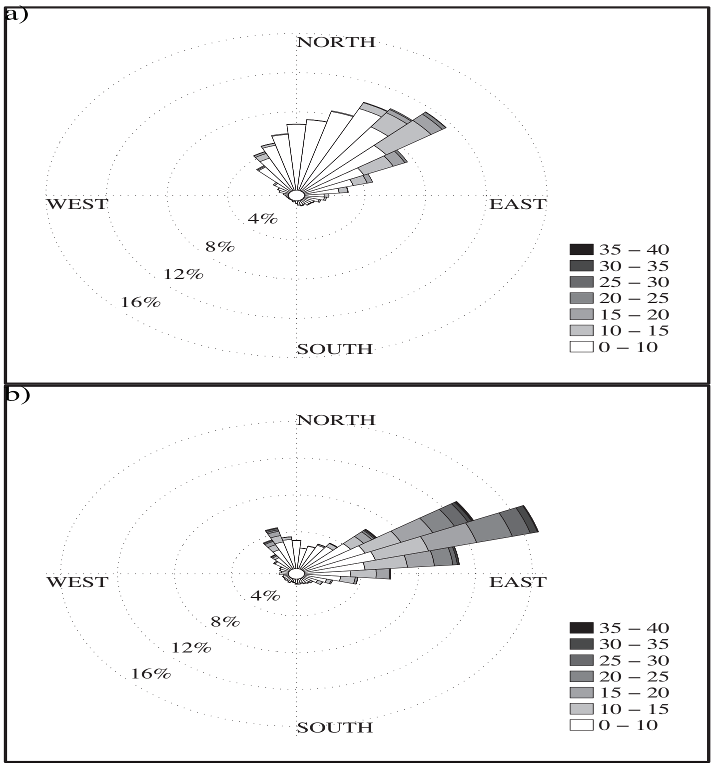

Fig. 3 The wind rose of the surface wind (m/s) during winter at Tasiilaq (near Sermilik Fjord) as represented in the: (a) ERA-I and (b) the ASR-I.

able to capture details of the coastal wind field as compared to the ERA-I. Figure 3 shows the wind roses at Tasiilaq as represented in the ERA-I and ASR-I. The ERA-I (Fig. 3a) clearly captures the prevalent northeasterly flow in the region that is associated with the barrier winds and there exists evidence of a clockwise turning of the winds towards northwesterly. The ASR-I (Fig. 3b) also captures this prevalence of barrier flow, albeit with slightly different directional characteristics. In contrast to the ERA-I, the ASR-I also includes a distinct secondary maximum for northwesterly flow that is representative of katabatic flow in the region.

As has been described in this article, the topographically forced weather systems that occur in southeast Greenland play an important role in the regional weather and climate. The changing nature of the climate in the region, such as the warming of the ocean and the retreat in sea ice, may have resulted in modifications of these weather systems. These systems are all strongly impacted by the nature of the storms that pass through the region and changes to their frequency, intensity or track can also impact these winds and their impact on the climate. The data sparse nature of the region and its complex topography along with the mesoscale nature of these topographic jets makes it a challenge to study them. As a result, atmospheric reanalyses have played a crucial role in their characterization. Reanalyses with sufficient resolution to capture the mesoscale nature of these weather systems are now becoming available. As described in this article, new and potentially important details on their structure are now becoming clear. For example, higher speed barrier flow tends to occur in regions where there are coastal ridges; while katabatic flow is absent from these regions and is focused into the fjords that typically occur along the sides of these ridges. Caution must however be expressed because many features of these weather systems are strongly influenced by the parameterizations that are part of the underlying data assimilation systems. Without a control for these influences, it is a challenge to assess the improvement in the representation of these weather systems that arises from increased horizontal resolution. As was found to be the case in the vicinity of Sermilik Fjord (Oltmanns et al. 2014), the availability of meteorological data in regions that are more representative of these weather systems, as opposed to the current stations that have a fair weather bias, would be of benefit in reducing the uncertainty as to their structure and impact.

References

Amundson, J.M., M. Fahnestock, M. Truffer, J. Brown, M.P. Lüthi, and R. J. Motyka, 2010: Ice melange dynamics and implications for terminus stability, Jakobshavn Isbrae Greenland. *J. Geophys. Res.-Earth Surf.*, **115,** F01005.

Arrigo, K.R., 2007: Chapter 7 physical control of primary productivity in Arctic and Antarctic polynyas. *Polynyas: windows to the worlds oceans*, W.O. Smith and D.G. Barber, Eds., Elsevier, Amsterdam, 223-238.

Barstad, I., and S. Gronas, 2005: Southwesterly flows over southern Norway - mesoscale sensitivity to large-scale wind direction and speed. *Tellus Ser. A*, **57**, 136-152.

Bromwich, D.H., and D.D. Kurtz, 1984: Katabatic wind forcing of the Terra-Nova Bay Polynya. *J. Geophys. Res.: Oceans*, **89,** 3561-3572.

Bromwich, D.H., et al., 2014: Contrasting the regional Arctic System Reanalysis with the global ERA-Interim Reanalysis. *Q.J.R. Meteor. Soc.*, submitted.

Cappelen, J., P.V. Jørgensen, E.V. Laursen, L.S. Stanius, and R.S. Thomsen, 2001: *The observed climate of Greenland, 1958-99 – with climatological standard normals. 1961-90.* Technical Report 00-18, Danish Meterological Institute, 154p.

Condron, A., and I.A. Renfrew, 2013: The impact of polar mesoscale storms on northeast Atlantic Ocean circulation. *Nat. Geosci.*, **6,** 34-37.

Daniault, N., P. Lherminier, and H. Mercier, 2011: Circulation and transport at the southeast tip of Greenland. *J. Phys. Oceanogr.* **41**, 437-457.

Dee, D. P., et al., 2011: The ERA-Interim reanalysis: configuration and performance of the data assimilation system. *Q.J.R. Meteor. Soc.*, **137**, 553-597.

Doyle, J.D., and M.A. Shapiro, 1999: Flow response to large-scale topography: The Greenland tip jet. *Tellus Ser. A*, **51**, 728-748.

DuVivier, A.K., and J.J. Cassano, 2013: Evaluation of WRF model resolution on simulated mesoscale winds and surface fluxes near Greenland. *Mon. Wea. Rev.*, **141**, 941-963.

Haine, T.W.N., S. Zhang, G.W.K. Moore, and I.A. Renfrew, 2009: On the impact of high-resolution, high-frequency meteorological forcing on Denmark Strait ocean circulation. *Q.J.R. Meteor. Soc.*, **135**, 2067-2085.

Harden, B.E., and I.A. Renfrew, 2012: On the spatial distribution of high winds off southeast Greenland. *Geophys. Res. Lett.*, **39,** L14806.

Harden, B.E., I.A. Renfrew, and G.N. Petersen, 2011: A climatology of wintertime barrier winds off southeast Greenland. *J. Climate*, **24**, 4701-4717.

Heinemann, G., 1999: The KABEG'97 field experiment: An aircraft-based study of katabatic wind dynamics over the Greenland ice sheet. *Bound.-Layer Meteor.*, **93**, 75-116.

Hocking, C., 1969: Dictionary of disasters at sea during the age of steam. Lloyd's Register of Shipping, London, 493 p.

Hoskins, B.J., and K.I. Hodges, 2002: New perspectives on the Northern Hemisphere winter storm tracks. *J. Atmos. Sci.*, **59**, 1041-1061.

Howat, I.M., Y. Ahn, I. Joughin, M.R. van den Broeke, J.T.M. Lenaerts, and B. Smith, 2011: Mass balance of Greenland's three largest outlet glaciers, 2000-2010. *Geophys. Res. Lett.*, **38,** L12501.

Klein, T., and G. Heinemann, 2002: Interaction of katabatic winds and mesocyclones near the eastern coast of Greenland. *Meteor. Applic.*, **9**, 407-422.

Laffineur, T., C. Claud, J.-P. Chaboureau, and G. Noer, 2014: Polar lows over the Nordic Seas: improved representation in ERA-Interim compared to ERA-40 and the impact on downscaled simulations. *Mon. Wea. Rev.*, in press.

Liu, A.Q., G.W.K. Moore, K.Tsuboki, I.A. Renfrew, 2006: The effect of the sea-ice zone on the development of boundary-layer roll clouds during cold air outbreaks, *Bound-Layer Meteor.*, **118**, 557-581.

Mills, B.J., and M.R. Anderson, 2003: Monitoring a piteraq storm system using DMSP imagery and Quikscat wind data. Preprints, *12th Conf. on Satellite Meteorology and Oceanography*, *Long Beach, CA*, American Met. Soc.

Moore, G.W.K., 2003: Gale force winds over the Irminger Sea to the east of Cape Farewell, Greenland. *Geophys. Res. Lett.*, **30,** 1894.

Moore, G.W.K., 2012: A new look at Greenland flow distortion and its impact on barrier flow, tip jets and coastal oceanography. *Geophys. Res. Lett.*, **39,** L22806.

Moore, G.W.K., and I.A. Renfrew, 2005: Tip jets and barrier winds: A QuikSCAT climatology of high wind speed events around Greenland. *J. Climate*, **18**, 3713-3725.

Murray, T., et al., 2010: Ocean regulation hypothesis for glacier dynamics in southeast Greenland and implications for ice sheet mass changes. *J. Geophys. Res.: Earth Surf.*, **115**, F03026.

Oltmanns, M., F. Straneo, G.W.K. Moore, S.H. Mernild, 2014: Strong downslope wind events in Ammassalik, southeast Greenland. *J. Climate*, **27**, 977-993.

Petersen, G.N., and I.A. Renfrew, 2009: Aircraft-based observations of air-sea fluxes over Denmark Strait and the Irminger Sea during high wind speed conditions. *Q.J.R. Meteor. Soc.*, **135**, 2030-2045.

Pickart, R.S., M.A. Spall, M.H. Ribergaard, G.W.K. Moore, and R.F. Milliff., 2003a: Deep convection in the Irminger Sea forced by the Greenland tip jet. *Nature*, **424**, 152-156.

Pickart, R.S., F. Straneo, and G.W.K. Moore, 2003b: Is Labrador Sea Water formed in the Irminger basin? *Deep-Sea Res. Part I*, **50,** 23-52.

Rasmussen, L., 1989: Greenland winds and satellite imagery. *Vejret-Danish Meteor. Soc.*, 32-37.

Renfrew, I.A., et al., 2008: The Greenland flow distortion experiment. *Bull. Am. Meteor. Soc.*, **89**, 1307-1324.

Renfrew, I.A., S.D. Outten, and G.W.K. Moore, 2009: An easterly tip jet off Cape Farewell, Greenland. I: Aircraft observations, *Q.J.R. Meteor. Soc.*, **135**, 1919-1933.

Sampe, T., and S.P. Xie, 2007: Mapping high sea winds from space: A global climatology. *Bull. Am. Meteor. Soc.*, **88**, 1965–1978.

Skamarock, W.C., 2004: Evaluating mesoscale NWP models using kinetic energy spectra. *Mon. Wea. Rev.*, **132**, 3019-3032.

Straneo, F., G.S. Hamilton, D.A. Sutherland, L.A. Stearns, F. Davidson, M.O. Hammil, G.B. Stenson, and A. Rosing-Asvids, 2010: Rapid circulation of warm subtropical waters in a major glacial fjord in East Greenland. *Nat. Geosci.,* **3**, 182-186.

Våge, K., T. Spengler, H.C. Davies, and R.S. Pickart, 2009: Multi-event analysis of the westerly Greenland tip jet based upon 45 winters in ERA-40. *Q.J.R. Meteor. Soc.*, **135**, 1999-2011.

Walter, J.I., J. E. Box, S. Tulaczyk, E. E. Brodsky, I. M. Howat, Y. Ahn, and A. Brown, 2012: Oceanic mechanical forcing of a marine-terminating Greenland glacier, *Ann. of Glaciol.*, **53**, 181-192.